Transient ion fluxes, driven by an external electric field in a thin electrolytic cell with blocking electrodes

2005 J. Phys.: Condens. Matter 17 1225

(http://iopscience.iop.org/0953-8984/17/7/015)

INSTITUTE OF PHYSICS PUBLISHING JOURNAL OF PHYSICS: CONDENSED MATTER

J. Phys.: Condens. Matter **17** (2005) 1225–1238 doi:10.1088/0953-8984/17/7/015

Transient ion fluxes, driven by an external electric field in a thin electrolytic cell with blocking electrodes

N Tankovsky and E Syrakov

Sofia University, Faculty of Physics, 5 James Bourchier Boulevard, Sofia-1164, Bulgaria

E-mail: tank@phys.uni-sofia.bg

Received 4 October 2004, in final form 8 December 2004
Published 4 February 2005
Online at stacks.iop.org/JPhysCM/17/1225

Abstract

A numerical algorithm is developed to examine the transient processes in an electrolytic cell with blocking electrodes when an external electric field is switched on and switched off stepwise in time. The algorithm is applicable for arbitrary mobilities and valence numbers of the ions and for large electric potentials, but is limited at present to small cell thickness, up to about 20 D lengths. The ion charge fluxes and the displacement current contributing to the total current in the cell have been evaluated and analysed. The ion charge behaviour in the linear approximation regime (low excitation voltage) and nonlinear regime (high voltage) have been compared. The dependences of the polarization and diffusion relaxation times on the ion parameters (valence and mobility), on the cell length and on the external electric potential are studied.

1. Introduction

The problems concerning the conductivity of intrinsic or extrinsic charge carriers, the frequency response of the material to an external electric field, the charge polarization and the capacitance of the diffuse double layer in the vicinity of the electrodes have been studied extensively, both in electrolytes [1–3] and in semiconductors [4, 5]. The transient processes in an electrode/electrolyte/electrode system, in response to external electric voltage, play an important role in different experimental electrochemical methods [6, 7]. However, the interpretation of the experimental results needs a theoretical basis capable of modelling different systems and conditions. The analysis of the dynamics of the ion charges in electrolyte, in response to high external voltage, requires a numerical treatment since the governing equations are nonlinear and do not allow us to obtain analytical solutions in a closed form. Franceschetti and MacDonald [8] have used the finite-difference approach and the general equations have been modified with the help of a fitting parameter. In a finite-element approach [9] the solution is found as a sum of localized functions with coefficients defined by minimization of one or more integrals. In the present work we have developed a numerical

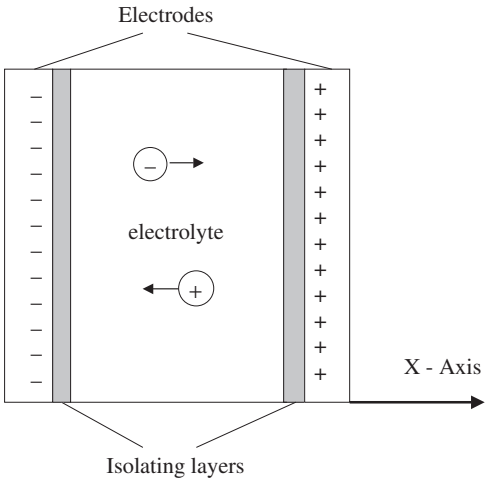

Figure 1. Electrolytic cell with blocking electrodes.

algorithm in which the nonlinearity terms are approximated by a small, one-time-step shift of one of the variables. The purpose of the present numerical analysis is to examine the transient ion fluxes and the total current in the cell, driven by a step voltage. The comparison of the transient processes in the linear regime at low excitation voltage with the nonlinear behaviour at high voltages is also interesting. We want to know also how the transients are influenced by the characteristic parameters of the solution, of the external electric field and of the electrolytic cell.

2. General equations

We shall consider an electrolytic cell comprising two parallel-plate electrodes, isolated by thin dielectric layers, as shown in figure 1. In this way the electrodes are blocking, i.e. no Faradaic currents occur through the electrode interfaces. The ion fluxes are due only to migration currents driven by an external electric field and opposed by diffusion processes. Assuming that only variations normal to the electrodes are present we can use one-dimensional description of the system, where X is the coordinate normal to the electrodes of the cell. We shall make some additional assumptions, which simplify the problem. We consider the solution to be a strong electrolyte of low concentration, i.e. the dissociation of the ions is complete and the charge recombinations and the interionic interactions can be neglected.

The general equations describing the transient processes in the electrolytic cell are the following [10]:

$$\frac{\partial n}{\partial t} = \frac{\partial}{\partial x}\left(D_n \frac{\partial n}{\partial x} + \mu_n n E\right) \tag{1}$$

$$\frac{\partial p}{\partial t} = \frac{\partial}{\partial x}\left(D_p \frac{\partial p}{\partial x} - \mu_p p E\right) \tag{2}$$

$$\frac{\partial E}{\partial x} = \frac{4\pi e}{\varepsilon}(Z_p p - Z_n n). \tag{3}$$

Here $n(x,t)$ and $p(x,t)$ are the negative and positive ion density distributions varying with time t, while $E(x,t)$ is the space and time dependence of the electric field. These are the

three functions to be defined from the set of equations (1)–(3). The diffusion coefficient, the mobility and the valence of the ions are denoted by D_i, μ_i and Z_i correspondingly, where $i = p$ for the positive ions and $i = n$ for the negative ions. The dielectric constant is denoted by ε and the protonic charge is given by e.

Another assumption, usually accepted, is the validity of the general Einstein–Nernst relation [10]:

$$\frac{kT}{eZ_i}\mu_i = D_i; \qquad i = n, p. \tag{4}$$

The positive and negative ion flux densities are defined by the Nernst–Planck equations as follows:

$$\begin{aligned} J_p &= D_p\frac{\partial p}{\partial x} - \mu_p pE \\ J_n &= D_n\frac{\partial n}{\partial x} + \mu_n nE. \end{aligned} \tag{5}$$

A measurable quantity, deserving evaluation, is the total current comprising the Faradaic flux components of the two types of ion charges and the displacement current:

$$I = Z_p eJ_p - Z_n eJ_n + \frac{\varepsilon}{4\pi}\frac{\partial E}{\partial t}. \tag{6}$$

Next we shall make all variables dimensionless by using the following normalization relations:

$$\begin{aligned} n^* &= \frac{nZ_n}{c_0}; \qquad p^* = \frac{pZ_p}{c_0}; \qquad E^* = \left(\frac{eL_\mathrm{D}}{kT}\right)E; \\ x^* &= \frac{x}{L_\mathrm{D}}; \qquad t^* = \frac{t}{\tau_\mathrm{D}}; \qquad I^* = \frac{L_\mathrm{D}I}{kTc_0(\mu_n+\mu_p)} \end{aligned} \tag{7}$$

where $c_0 = Z_n n_0 = Z_p p_0$ is the uniform, unperturbed charge concentration obeying the overall electroneutrality condition, k is the Boltzmann constant, T is the temperature, L_D is the Debye length and τ_D is the dielectric relaxation time, defined by the following formulae:

$$L_\mathrm{D}^2 = \frac{\varepsilon kT}{4\pi e^2(Z_n^2 n + Z_p^2 p)} = \frac{\varepsilon kT}{4\pi e^2 c_0(Z_n + Z_p)} \tag{8}$$

$$\tau_\mathrm{D} = \frac{\varepsilon}{4\pi e(Z_n n\mu_n + Z_p p\mu_p)} = \frac{\varepsilon}{4\pi e c_0(\mu_n+\mu_p)}. \tag{9}$$

In this way the space coordinate is scaled to the Debye length and the time scaling is the dielectric relaxation time. We denote the electrolytic cell thickness by L and we take the integration range from $x = -L/2$ to $L/2$. Correspondingly, for the dimensionless coordinate x^* the cell thickness is $2M$ and the integration range is from $x^* = -M$ to M, where M is the number of Debye lengths in a cell half-length i.e. $M = L/2L_\mathrm{D}$. For a highly diluted solution $L_\mathrm{D} \cong 10^{-8}$ m and if we take the cell length $L \cong 10^{-3}$ m we get $M \cong 10^5$.

Taking into account (7)–(9) and substituting (7) into (1)–(3) we obtain the following dimensionless variant of the general system of equations:

$$\frac{\partial n^*}{\partial t^*} = \frac{\pi_\mathrm{m}}{1+\pi_\mathrm{m}}\left(\frac{Z_n+Z_p}{Z_n}\right)\frac{\partial}{\partial x^*}\left(\frac{\partial n^*}{\partial x^*} + Z_n n^* E^*\right) \tag{10}$$

$$\frac{\partial p^*}{\partial t^*} = \frac{1}{1+\pi_\mathrm{m}}\left(\frac{Z_n+Z_p}{Z_p}\right)\frac{\partial}{\partial x^*}\left(\frac{\partial p^*}{\partial x^*} - Z_p p^* E^*\right) \tag{11}$$

$$\frac{\partial E^*}{\partial x^*} = \frac{p^* - n^*}{Z_n + Z_p} \tag{12}$$

where

$$\pi_{\mathrm{m}} = (\mu_n/\mu_p) \tag{13}$$

is the ratio of the mobility of the negative to the mobility of the positive ions.

It can be noticed that the values of all the dimensionless coefficients appearing in the set of equations (10)–(12) are of first order of magnitude, while the only high value number for a real macrosystem is the integration range $2M$.

For simplicity of writing, we shall omit further the asterisks in (10)–(12), but we shall remember that all the variables are dimensionless and are normalized in agreement with (7).

Next we introduce three new variables, which will be useful to decompose each second order differential equation into a couple of first order differential equations. These dimensionless variables are the negative ion flux $N(x, t)$, the positive ion flux $R(x, t)$ and the electric potential $Y(x, t)$, defined as follows:

$$N = \frac{\partial n}{\partial x} + Z_n n E \tag{14}$$

$$R = \frac{\partial p}{\partial x} - Z_p p E \tag{15}$$

$$E = -\frac{\partial Y}{\partial x}. \tag{16}$$

Taking into account (14)–(16) we obtain from (10)–(12) the following set of six first-order differential equations:

$$\frac{\partial N}{\partial x} = \left(\frac{1+\pi_{\mathrm{m}}}{\pi_{\mathrm{m}}}\right)\left(\frac{Z_n}{Z_n + Z_p}\right)\frac{\partial n}{\partial t} \tag{17}$$

$$\frac{\partial n}{\partial x} = N - Z_n n E \tag{18}$$

$$\frac{\partial R}{\partial x} = (1+\pi_{\mathrm{m}})\left(\frac{Z_p}{Z_n + Z_p}\right)\frac{\partial p}{\partial t} \tag{19}$$

$$\frac{\partial p}{\partial x} = R + Z_p p E \tag{20}$$

$$\frac{\partial E}{\partial x} = \frac{p - n}{Z_n + Z_p} \tag{21}$$

$$\frac{\partial Y}{\partial x} = -E. \tag{22}$$

The dimensionless total current can be defined from (6) and (7) as follows:

$$I = \frac{R}{1+\pi_{\mathrm{m}}} - \frac{N}{1+\pi_{\mathrm{m}}^{-1}} + \frac{\partial E}{\partial t}. \tag{23}$$

We assume that the electric potential is switched on infinitely fast at $t = 0$. Then we have the following initial conditions for the above system of equations:

$$n(x, t=0) = 1; \qquad p(x, t=0) = 1; \qquad Y(x, t=0) = \frac{Bx}{M} \tag{24}$$

where $B = eY_0/kT$ is the dimensionless electric potential. Immediately after the electric field is switched on and before the ions are rearranged by migration and diffusion, the potential Y has a linear dependence over x, as in a dielectric.

Four boundary conditions express the fact that the electrodes are blocking and hence the ion fluxes N and R are zero at both boundaries:

$$N(x=-M, t) = N(x=M, t) = R(x=-M, t) = R(x=M, t) = 0. \tag{25}$$

Two other boundary conditions show that the external electric potential is kept constant in time at the two boundaries:

$$Y(x = -M, t) = -B; \qquad Y(x = M, t) = B. \tag{26}$$

3. Numerical algorithm

Equations (17)–(22) define a set of nonlinear partial differential equations which can be approached analytically only in the framework of some simplifying assumptions, e.g. a linear approximation when the electric forces are much smaller than the thermal perturbations, i.e. for $B \ll 1$. In the nonlinear case for large electric voltage, i.e. for $B > 1$, a numerical treatment is necessary, which gives us the possibility to analyse a wide variety of parameters and situations.

If we shift the electric field $E(x, t)$ by one time step relative to the charge densities $n(x, t)$ and $p(x, t)$, then we can linearize the right-hand terms in equations (18) and (20). Thus, the set of coupled equations (17)–(22) can be decomposed into independent pairs of linear equations as follows: equations (17) and (18) define $n(x, t)$ and $N(x, t)$, (19) and (20) define $p(x, t)$ and $R(x, t)$, while (21) and (22) define $E(x, t)$ and $Y(x, t)$. This can be done in two ways.

(1) One way is to take $E(x, t - \Delta t)$ in (18) and (20) as a known function of x, determined in the previous time step. After having found in this way $n(x, t)$ and $p(x, t)$ we substitute them in (21) and find $E(x, t)$.
(2) An alternative way is to take $n(x, t - \Delta t)$ and $p(x, t - \Delta t)$ as known functions, found in the previous time step, and then find $E(x, t)$ in (21). Later, substituting $E(x, t)$ in (17)–(20) we can find $n(x, t)$ and $p(x, t)$.

Both schemes give similar results, so for convenience we have used the second one. For an arbitrary function $f(x, t)$ we accept the following rule of discretizing the time and the space:

$$f(x, t) = f_i^k(x_i, t_k). \tag{27}$$

If we denote the space step by h and the time step by τ the algorithm can be presented in a general form as follows:

$$\frac{E_{i+1}^k - E_i^k}{h} = \frac{p_i^{k-1} - n_i^{k-1}}{Z_n + Z_p} \tag{28}$$

$$\frac{Y_{i+1}^k - Y_i^k}{h} = -E_i^k \tag{29}$$

$$\frac{N_{i+1}^k - N_i^k}{h} = \left(\frac{Z_n}{Z_n + Z_p}\right)(1 + \pi_{\mathrm{m}}^{-1})\left(\frac{n_i^k - n_i^{k-1}}{\tau}\right) \tag{30}$$

$$\frac{n_{i+1}^k - n_i^k}{h} = N_i^k - Z_n n_i^k E_i^k \tag{31}$$

$$\frac{R_{i+1}^k - R_i^k}{h} = \left(\frac{Z_p}{Z_n + Z_p}\right)(1 + \pi_{\mathrm{m}})\left(\frac{p_i^k - p_i^{k-1}}{\tau}\right) \tag{32}$$

$$\frac{p_{i+1}^k - p_i^k}{h} = R_i^k + Z_p p_i^k E_i^k. \tag{33}$$

An outer iteration loop is used to scan the values over the time steps (indexes k), while inner loops calculate the space distributions (indexes i) at a fixed time. The derivatives in equations (28)–(33) are presented in a general Euler formulation. Actually E and Y in equations (28) and (29) are integrated by the Simpson rule, while n, N, p and R in equations

(30)–(33) are calculated by the fourth-order Runge–Kutta method. The boundary conditions are taken into account with the help of the 'shooting method' [11].

Theoretical estimation of the dependence of the stability of the algorithm on the parameters of the system appeared to be a difficult task, so we have examined the stability empirically. We have used uniform discretizing meshes in the space and time coordinates and we have obtained stable results for systems as large as $M \leqslant 50$. A potential improvement of the algorithm can be obtained if we use, as done in [8], logarithmically changing space steps, smaller in the vicinity of the electrodes where amplitudes are growing rapidly and larger steps about the centre of the cell, where the amplitudes are smaller. Analogously, logarithmically decreasing time steps, larger at the beginning, when the deviations from equilibrium are small, and smaller time steps at later moments, would improve the performance of the algorithm.

4. Results and discussions

We shall examine firstly the transient processes in the solution when a constant external electric potential is switched on stepwise in time. We consider a relatively thin cell ($M = 6$) and symmetric electrolyte when both types of ions have equal valence numbers $Z_n = Z_p = 1$ and equal mobility $\pi_{\mathrm{m}} = 1$. We shall compare the time–space evolution of the system in two cases: in the quasi-linear regime when $B \ll 1$ and in the nonlinear regime when $B > 1$. The obtained positive charge space-distributions $p(x, t)$ for $B = 0.1$, i.e. linear behaviour, are presented graphically in figure 2(a) at four consecutive moments in time. The same curves are shown for $B = 4$, i.e. nonlinear behaviour in figure 2(b). The negative charge distribution curves $n(x, t)$ are symmetrical to the curves $p(x, t)$, relative to the cell centre at $x = 0$, and will not be shown to avoid overloading of the pictures.

It can be noticed that in the linear regime, for low excitation voltages (figure 2(a)), the charge density perturbations, adjacent to the two electrodes, are almost identical. The depletion and the polarization regions are preserved symmetrical in time. In the nonlinear case (figure 2(b)) the curves have a different character in the two interfacial regions adjacent to the electrodes. The ion charges in the polarization region i.e. at the electrode of opposite charge (left-hand side in figure 2(b)) grow high with time, but the resultant electrical double layer preserves a constant thickness, about one Debye length. The curves obtained when the system, evolving in time, approaches equilibrium ($t = 4$ in figures 2(a) and (b)) can be compared with the nonlinear Poisson–Boltzmann density distribution, which in the notations of the considered system can be written as follows:

$$\begin{aligned} p(x) &= \exp\left(-4ath\left(th\left(\frac{B}{4}\right)\exp(-x)\right)\right) \\ n(x) &= \exp\left(4ath\left(th\left(\frac{B}{4}\right)\exp(-x)\right)\right). \end{aligned} \tag{34}$$

The distributions (34) can be obtained when the solution for the potential of the Poisson–Boltzmann equation is substituted in the Boltzmann charge density distribution [12]. Formulae (34) are valid for all values of the potential B, but are limited only for a static regime, for a single electrode and for the case of a symmetrical 1-1 electrolyte. The dependences (34) are presented graphically with dotted lines in figure 3(a) for $B = 0.1$ and in figure 3(b) for $B = 4$. It can be noticed that for weak electrical perturbations ($B = 0.1$) the theoretical dotted line curves in figure 3(a) coincide well with the continuous line curves, obtained from the simulation in a thin cell ($M = 6$) in figure 2(a) for $t = 4$. For high electrical potentials ($B = 4$) a discrepancy occurs between the theoretical dotted line curves in figure 3(b) and the continuous line curves for $t = 4$ in figure 2(b), which is due to the fact that the simulation

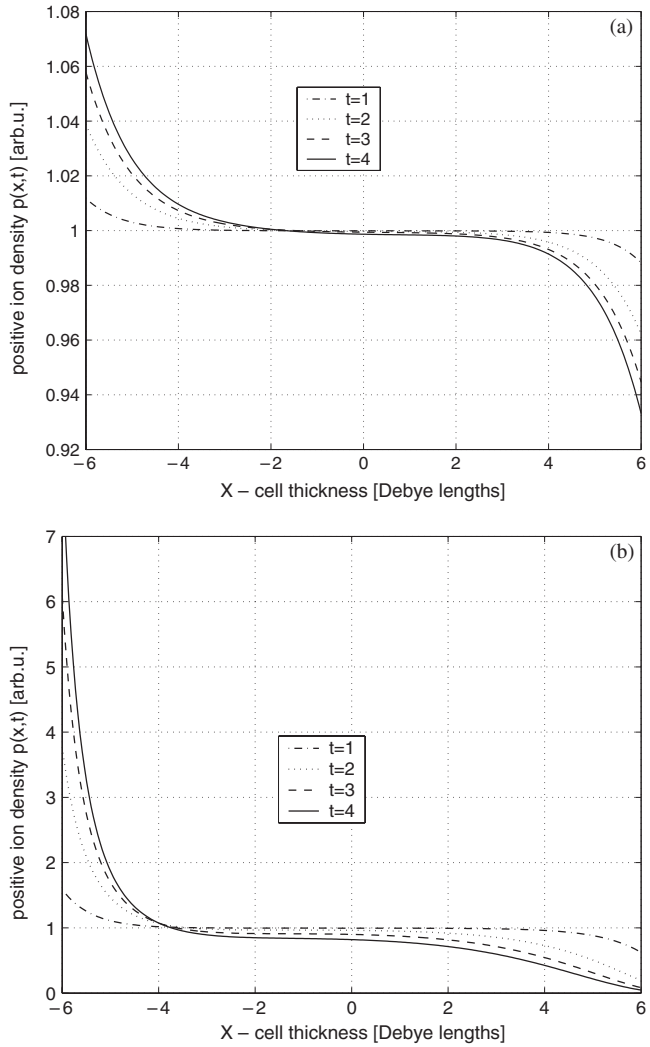

Figure 2. Transient polarizing evolution of positive ion density $p(x, t)$ for symmetrical electrolyte when $Z_n = Z_p = 1$; $\pi_m = 1$; $M = 6$. (a) Linear behaviour for $B = 0.1$. (b) Nonlinear behaviour for $B = 4$.

curve is evaluated for a thin cell $M = 6$, while the theoretical curve is calculated for a single electrode i.e. $M \to \infty$. In the thin cell the number of ions is preserved constant, while in the infinitely thick cell the electroneutrality condition is obeyed only for the charges adjacent to the electrode.

The electrical potential space distributions $Y(x, t)$ are presented in figure 4(a) for $B = 0.1$ and in figure 4(b) for $B = 4$, in the same time sequence as in figure 2. There is almost no difference in the curves in both figures, but a slight tendency can be noticed that the electric potential is better screened by the ions for the low external potential (figure 4(a)) than for the high potential (figure 4(b)).

The time evolution of the space distribution of the positive ion flux $R(x, t)$ is shown in figure 5(a) for $B = 0.1$ and in figure 5(b) for $B = 4$. The curves of the negative ion flux

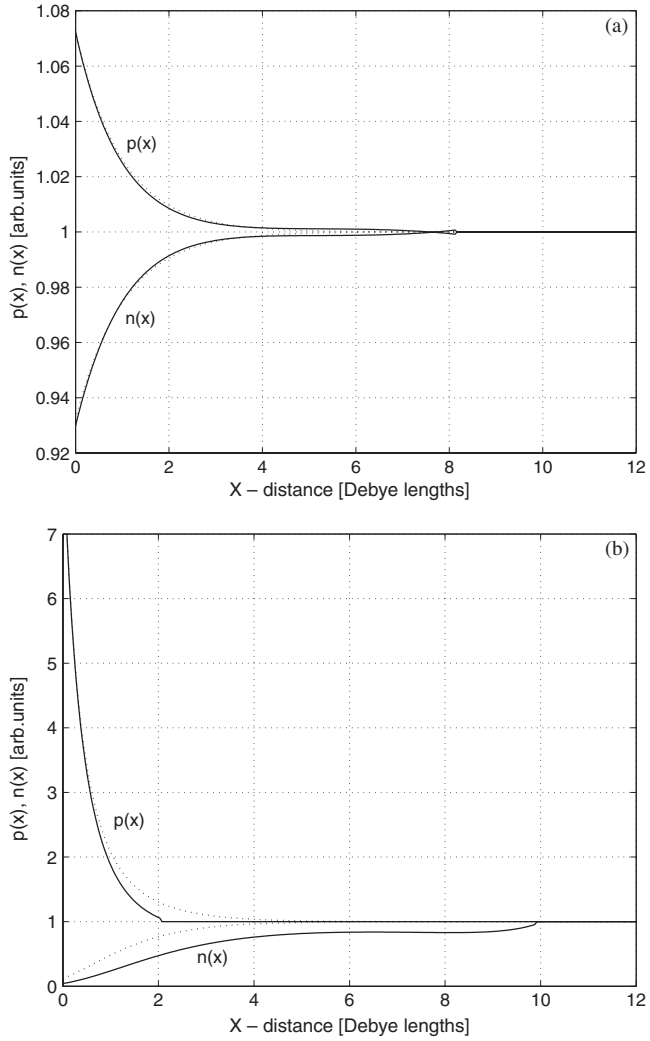

Figure 3. Positive $p(x)$ and negative $n(x)$ ion density for symmetrical electrolyte when $Z_n = Z_p = 1$; $\pi_m = 1$; dotted curves—the Poisson–Boltzmann distribution for an infinitely thick cell $M \to \infty$; continuous curves—simulation for a thin cell, $M = 6$ and for $t = 4$ in figure 2. (a) Linear behaviour for $B = 0.1$. (b) Nonlinear behaviour for $B = 4$.

$N(x, t)$ are symmetrical to the curves $R(x, t)$, relative to the cell centre at $x = 0$, and are not presented for simplicity. For the linear case presented in figure 5(a) the space distribution of the ion flux is preserved symmetrical in time. For the nonlinear case in figure 5(b) one can notice asymmetry of the space distribution of the ion flux varying with time. The flux stays larger in the polarization region (left side in figure 5(b)) and falls lower in the depletition region (right side in figure 5(b)). This is in agreement with the higher charge concentration gradients built next to the electrode of opposite charge as shown in figure 2(b).

We can conclude that in the low voltage approximation the transient processes in the vicinity of the two electrodes are symmetrical, while in the nonlinear approximation the transients of the charge carriers are essentially asymmetrical at the two electrodes.

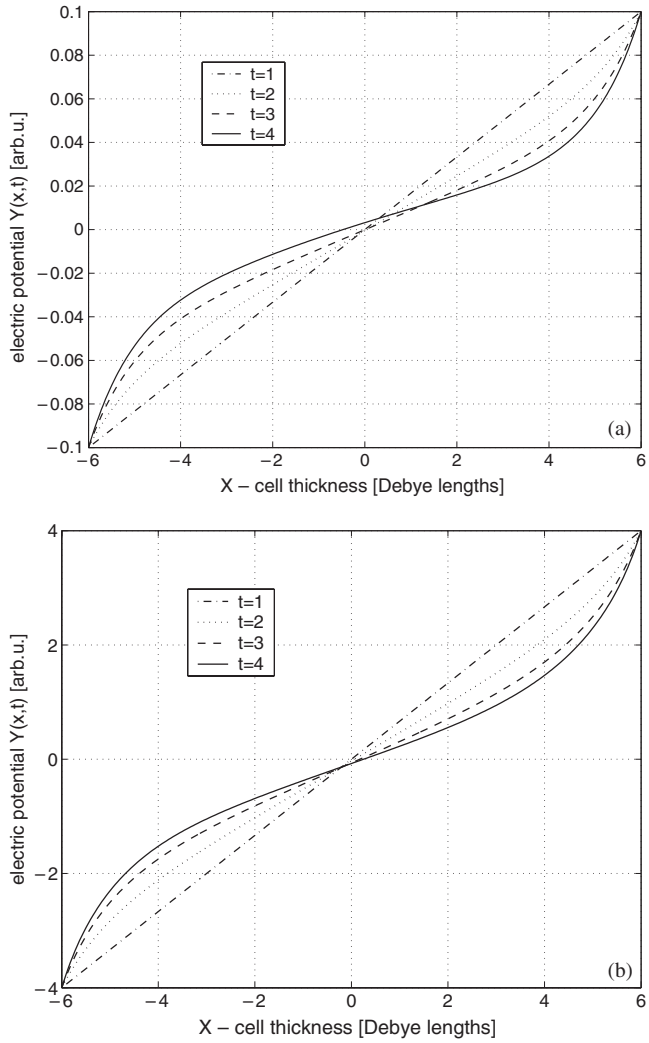

Figure 4. Time dependence of the electric voltage space distribution $Y(x, t)$ when $Z_n = Z_p = 1$; $\pi_m = 1$; $M = 6$. (a) Linear behaviour for $B = 0.1$. (b) Nonlinear behaviour for $B = 4$.

The time dependences of the negative and positive ion fluxes $N(t)$ and $R(t)$ for a symmetrical electrolyte, descending from maximum to zero when an equilibrium is achieved, are shown in figure 6(a). The dependence on x is eliminated by averaging over the cell length. We shall denote the specific times of the polarizing negative and positive ion fluxes with TP_n and TP_p, correspondingly. As a quantitative measure we choose the time intervals at half maximum of the curves $N(t)$ and $R(t)$. Obviously for the case when the two types of ions have the same valence and mobility we have $TP_n = TP_p$ as shown in figure 6(a).

When the mobility of the negative ions is bigger i.e. $\pi_m = 2$ the flux amplitude $N(t)$ of the faster negative ions is bigger and equilibrium is reached for a shorter time i.e. $TP_n < TP_p$, as shown in figure 6(b).

The displacement current was also evaluated numerically, but its amplitude appeared to be about three orders of magnitude smaller than the charge carrier Faradaic currents and hence its contribution to the total current is negligible.

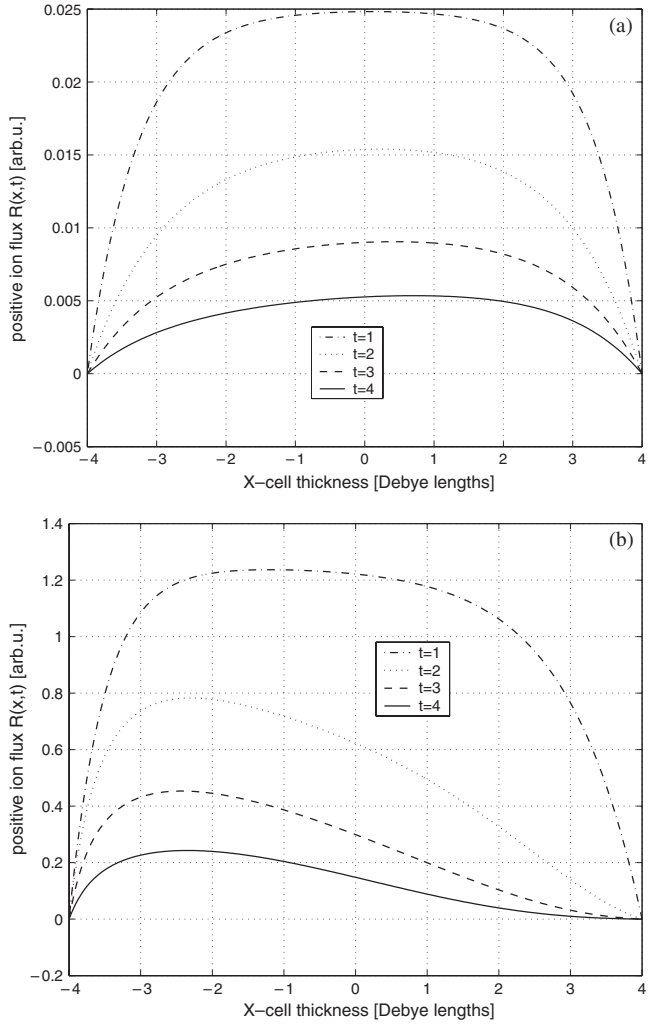

Figure 5. Time dependence of the positive ion flux $R(x, t)$ when $Z_n = Z_p = 1$; $\pi_m = 1$; $M = 6$. (a) Linear behaviour for $B = 0.1$. (b) Nonlinear behaviour for $B = 4$.

The Faradaic currents of the positive and negative ion charges can be calculated but cannot be separated experimentally. A measurable quantity is the total current and its evaluation from (23) is useful. The time dependence of the polarizing total current $I(t)$ is shown in figure 7(a) in a linear approximation for $B = 0.1$ and in figure 7(b) in a nonlinear regime for $B = 4$. The amplitudes are normalized to the maximum values for better comparison of the time dependences. The curves in figures 7(a) and (b) are almost identical besides the slightly smaller values of the relaxation times for $B = 4$ in comparison with the curves for $B = 0.1$.

We have also examined the dependence of the polarizing time on the electric potential B and on the cell length $L = 2M$. In figure 8 the dependence TP(B) is given for different values of M. It is shown that the curves TP(B) are almost flat. However, for thinner cells (small values of M) the curves TP(B) are descending continuously, while for thicker cells (higher values of M) the curves are almost horizontal with a small jump at higher voltages, i.e. in the nonlinear region. A numerical analysis carried out by Kahn and Maycock [13] has shown no

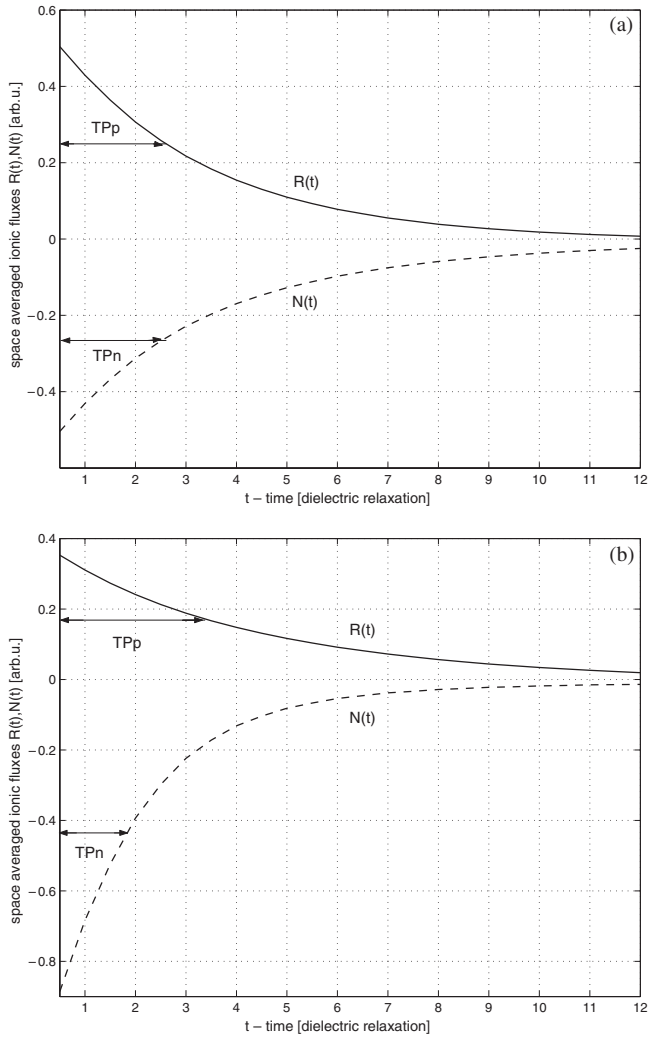

Figure 6. Time dependence of space-averaged positive and negative ion fluxes $R(t)$ and $N(t)$. (a) Equal ion mobilities $\pi_m = 1$. (b) Different ion mobilities $\pi_m = 2$.

dependence of TP on B in the region about $M > 10$ and $B < 2$, which is in accordance with the curves in figure 8. The numerical calculations of the authors in [8] found that 'the principal decay constant varies somewhat with B for $M = 10$ and 20, but not as much as in the $M = 1$ case'. This observation is also in a qualitative agreement with figure 8.

The dependence of the polarizing time on the cell thickness TP(M) is shown in figure 9 for a constant driving electric potential $B = 2$. Obviously in a thicker cell the equilibrium is reached in a larger time interval. However, a saturation tendency can be noticed for higher values of M.

The transient process of polarizing the electrodes is determined by ion migration, opposed by ion diffusion. We have found that the polarizing times TP depend on:

- the properties of the ions—ion mobility and ion valence
- the properties of the cell—cell length, measured in Debye lengths
- the strength of the external electric field.

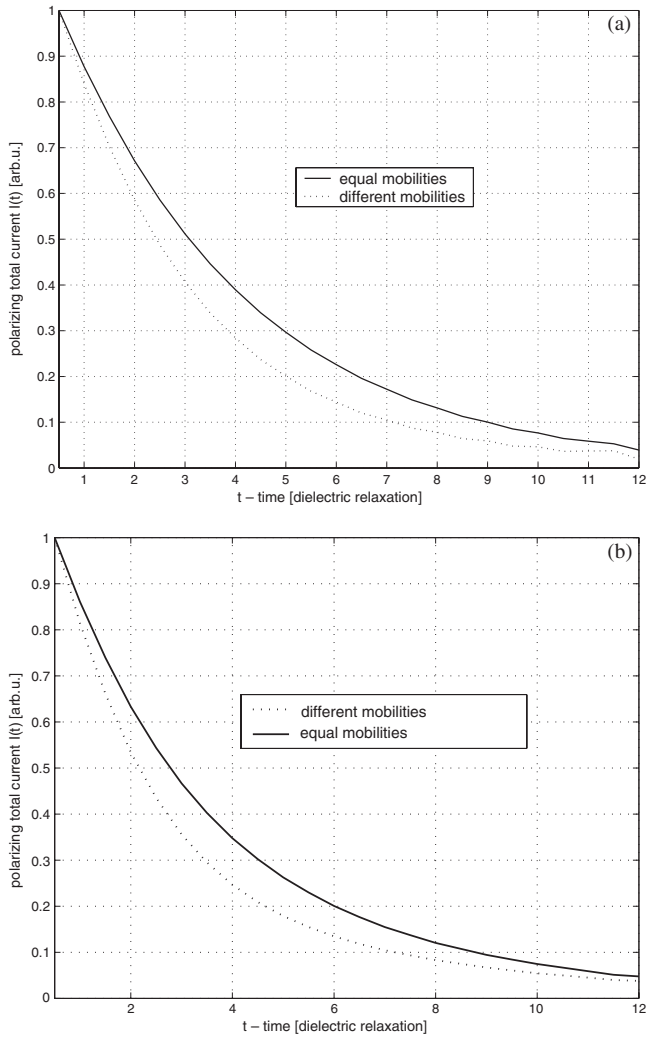

Figure 7. Time dependence of the polarizing total current $I(t)$ for equal mobilities $\pi_m = 1$ (continuous curves) and for different mobilities $\pi_m = 2$ (dotted curves). (a) Linear behaviour for $B = 0.1$. (c) Nonlinear behaviour for $B = 4$.

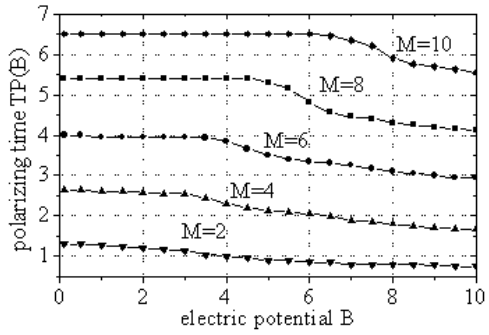

Figure 8. Dependence of the polarizing relaxation time on the external electric potential TP(B).

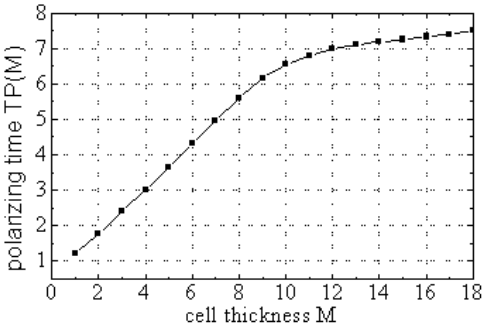

Figure 9. Dependence of the polarizing relaxation time on the cell thickness TP(M).

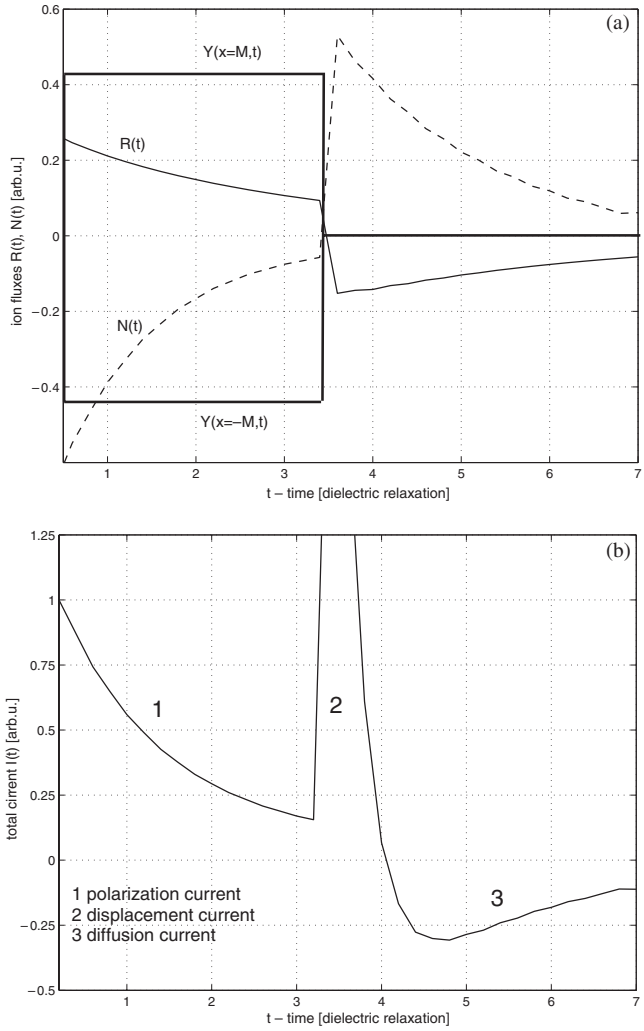

Figure 10. (a) Time dependence of the space-averaged positive and negative ion fluxes $R(t)$ and $N(t)$ for different ion mobilities $\pi_{\mathrm{m}} = 2$ when the external voltage varies stepwise as shown with thick continuous lines $Y(x = -M, t)$ and $Y(x = M, t)$. (b) Time dependence of the total current $I(t)$ for the same conditions as in figure 10(a).

Next we want to analyse the diffusion transient fluxes, when the electric field is switched off and only diffusion drives the polarized ion charges back to uniform space distribution. The time dependence of the external electric potential $Y(x = -M, t)$, $Y(x = M, t)$ at both electrodes is shown with thicker lines, while the transient positive and negative ion fluxes $R(t)$ and $N(t)$ are shown in figure 10(a) for the case of different ion mobilities ($\pi_m = 2$). The time dependence of the corresponding total current $I(t)$ is shown in figure 10(b). The high pulse observed in figure 10(b) at the moment when the external electric voltage is sharply shut down is due to the displacement current. We have already found that the displacement current is negligibly small for the slow time changes of the electric field caused by ion migration, but when the external voltage is varying fast the displacement current is dominant as seen in figure 10(b). It can be noticed that the relaxation times of both the diffusion total current and the polarization total current are a little higher than unity, which is the dielectric relaxation time, but of the same order of magnitude.

5. Conclusions

A numerical algorithm has been developed to examine the transient processes in a thin electrolytic cell. It has been shown that in the limit of low excitation voltage (linear approximation) the ion charge distributions and the ion fluxes are identical at the two electrodes, while for high voltages (nonlinear regime) the ion charges behave differently in the vicinity of the two electrodes. The time dependence of the total current in the cell, as well as its components—the Faradaic currents for the two types of ions and the displacement current, have been evaluated and analysed. It has been shown that in a thin cell the relaxation times of polarization and diffusion depend on the properties of the solution, but also on the cell-length and on the external electric field. Our analysis is restricted to relatively thin cells ($M < 20$), but in a future work we hope to develop the algorithm for the limiting case when $M \to \infty$.

References

[1] MacDonald J R 1969 *Trans. Faraday Soc.* **65** 943–58
[2] Buck R P 1969 *J. Electroanal. Chem.* **23** 219–40
[3] MacDonald J R 1974 *J. Electroanal. Chem.* **53** 1–55
[4] MacDonald J R 1958 *J. Chem. Phys.* **29** 1346–58
[5] Jaffe G 1952 *Phys. Rev.* **85** 354–63
[6] Galus Z 1976 *Fundamentals of Electrochemical Analysis* (New York: Halsted)
[7] Hunter R J 1998 *Colloids Surf.* A **141** 37–66
[8] Franceschetti D R and MacDonald J R 1979 *J. Appl. Phys.* **50** 291–302
[9] Norie D H and DeVries G 1973 *The Finite Element Method* (New York: Academic)
[10] MacDonald J R 1973 *J. Chem. Phys.* **58** 4982–5001
[11] Press W H, Teukolsky S A, Vetterling N T and Flannery B P 1992 *Numerical Recipes: The Art of Scientific Programming* (Cambridge: Cambridge University Press)
[12] Martinov G A and Salem R R 1983 *Lecture Notes in Chemistry* vol 33 (Berlin: Springer)
[13] Kahn D and Maycock J N 1967 *J. Chem. Phys.* **46** 4434